北見工業大学研究報告
第19巻 第1号 (昭和62年)

Memoirs of the Kitami Institute of Technology
Vol. 19 No. 1 (1987)

Global Relation Between the Steady State Rate Mode and the Transient State Behavior of Products*

by Hideaki KOBAYASHI**, Tohru KANNO***
and Masayoshi KOBAYASHI***

(Received April 30, 1987)

Abstract

A new approach has been applied to find the global relation between the mode of steady state rate function (SSF) and the transient state behavior (TSB), by using a computer simulation technique. A typical complex reaction model producing two different products in parallel in which a stable surface intermediate participant (In) is added is used as an example.

The mode of the SSF is classified into three typical types according to the values of the kinetic parameters employed; Type A: monotonous increase mode for the two products (lower surface coverage of (In), $\theta_{In}<0.1$); Type B: the volcano mode for one and the monotonous increase mode for another product (higher surface coverage of (In), $\theta_{In}=0.1$–0.7) and Type C: volcano mode for the two products ($\theta_{In}=0.1$–0.9). The modes were sensitively characterized by the amount of the surface intermediates and the kinetic parameters.

The TSB is drastically and sensitively varied depending on the combination of the values of kinetic parameters and the surface coverage of the adsorbed species relating to the mode of the SSF. The modes of TSB are classified into four characteristic types; Type I: Over-shoot mode which appears on a relatively lower surface coverage of (In) ($\theta_{In}<0.4$) plus the slower regeneration of active species (at the low concentration region of Types A and B); type II: False start mode which is observed with a relatively lower surface coverage of (In) (0.1–0.3) plus the inhibition effect of reactant (at the high concentration region of Type A and low concentration region of Type C); Type III: Extraordinarily slow response mode which appears on very slow reconfiguration of the adsorbed species (at the medium concentration region of Type C); Type IV: No change mode which results from the saturated coverage with the surface intermediates (at the high concentration region of Type C).

1. Introduction

In industrial engineering, a parallel consecutive reaction producing a useful intermediate is basically important. Olefine oxidation to produce epoxides, for example, has been considered as follows.[1~4]

Department of Industrial Chemistry, Kitami Institute of Technology 090 Kitami, Hokkaido, Japan.

* The paper was presented at the Hokkaido regional meeting of the Chemical Society of Japan in the winter period of 1986.

** Chemical Environmental Engineering.

*** Department of Industrial Chemistry.

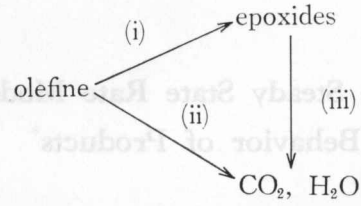

(1)

Generally speaking, one may divide equation (1) into two cases; (1) the parallel reaction involving steps (i) and (ii) at the low temperature region and (2) the parallel consecutive reaction involving steps (i), (ii) and (iii) at the high temperature region.

At the low temperature region, the catalyst surface is considerably covered by the large amounts of many kinds of adsorbed species. In particular, some stable surface intermediates (In) are accumulated on the surface in appreciable amounts as expressed in equation (2).[5~9]

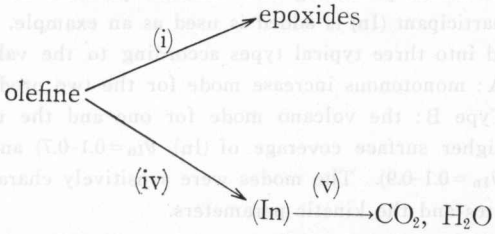

(2)

The surface coverage of (In) might play an important role in controlling the selectivity of epoxide production in the actual reactions. Based on our experimental results for ethylene oxidation, for example, the surface coverage of (In) falls in the range of $\theta_{In}=0.1-1.0$. In this case, the accumulation of the (In) characterizes a volcano type mode of the steady state rate function displayed by a function of the concentration of ethylene.

At the high temperature range, the catalyst surface is relatively free from the adsorbed species indicating a low surface coverage, and the atoms constituting the solid surface instead become mobile, which causes an enhancement of the reactivity of the adsorbed species. In this case, it is the activity of the adsorbed species that strongly controls the selectivity of the epoxides rather than the surface coverage of (In). Thus, the competitive reaction between steps (i), (ii) and (iii) is a key to characterize the mode of the SSF.

In our previous papers[10,11], we reported that the mode of the transient response curves of products caused by the step change in the concentration of reactants is drastically changed by the combination of kinetic parameters and the surface coverage of stable intermediates. The object of this study is to find a global relation between the modes of the SSF and the TSB, and to classify then into a visualized diagram.

For the computer simulation of transient response curves, a commercial personal computer (NEC, PC-8001mkII) was used, to which an arithmetic processing unit type AM9511 was attached so as to shorten the computing time.

2. Presentation of a Model

(1) Reaction Model

In the present study, ethylene oxidation over a silver catalyst is considered as a simple example of complex triangle reactions. Based on our experimental data of ethylene oxidation on Ag, a modified reaction model including a stable surface intermediate may be proposed as follows

$$\left.\begin{aligned} &A+\frac{1}{2}B_2\rightarrow R \\ &A+3B_2\rightarrow 2F+2G \end{aligned}\right\} \text{ overall reaction} \tag{3}$$

$$A(g)+B_2\cdot S\xrightarrow{k_1}R(g)+B\cdot S \tag{4}$$

$$A(g)+3B\cdot S\xrightarrow{k_2}\mathrm{In}\cdot 3S \tag{5}$$

$$\mathrm{In}\cdot 3S+2B_2\cdot S\xrightarrow{k_3}2F(g)+2G(g)+B\cdot S+4S \tag{6}$$

$$B_2(g)+S\xrightarrow{k_4}B_2\cdot S \tag{7}$$

$$A(g)+B\cdot S\underset{k_{-5}}{\overset{k_5}{\rightleftarrows}}A\cdot B\cdot S \tag{8}$$

$$B_2\cdot S+S\underset{k_{-6}}{\overset{k_6}{\rightleftarrows}}2B\cdot S \tag{9}$$

where (In) is a surface stable complex which consists of more than two species, and step (8) means an inhibition effect due to the adsorption of reactant A on the active species $B\cdot S$. This term is reasonably added based on the actual experimental data.

(2) Material Balance Equations

Let us consider a tubular flow reactor as illustrated in Fig. 1. For the mass balance of reactant A around the differential length dZ:[12]

$$\text{input by flow}: \frac{UA(s)\rho_M P_A}{\pi} \tag{10}$$

$$\text{output by flow}: \frac{A(s)\,\rho_M}{\pi}\left(P_A+\frac{\partial P_A}{\partial Z}\,dZ\right)\left(U+\frac{\partial U}{\partial Z}\,dZ\right) \tag{11}$$

$$\text{consumption by chemical reaction}: \left(k_1P_A\theta_{B_2}+k_2P_A\theta_B{}^3+k_5P_A\theta_B-k_{-5}\theta_{AB}\right)\rho_c A(s)\,dZ \tag{12}$$

$$\text{accumulation}: \rho_M\varepsilon A(s)\frac{\partial P_A}{\partial t}\,dZ \tag{13}$$

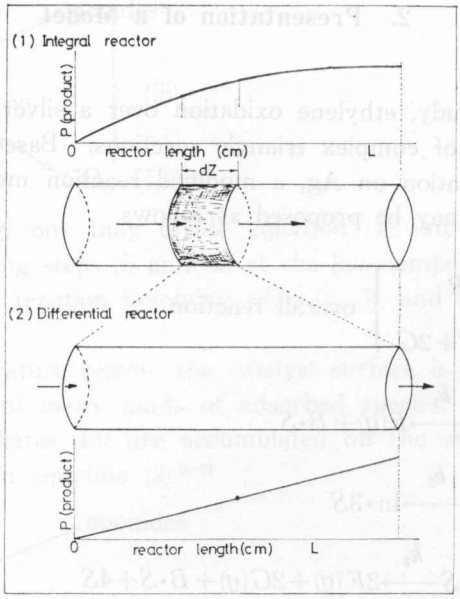

Fig. 1. Schematic explanation for the differential reactor model.

Equating the difference in input/output terms to accumulation in the volume element $A(s)dZ$ gives

$$-\frac{1}{\rho_c R_g T}\left(U\frac{\partial P_A}{\partial Z}+P_A\frac{\partial U}{\partial Z}\right)-(k_1 P_A\theta_{B_2}+k_2 P_A\theta_B{}^3+k_5 P_A\theta_B-k_{-5}\theta_{AB})$$
$$=\frac{\varepsilon}{\rho_c R_g T}\frac{\partial P_A}{\partial t} \tag{14}$$

The change in the gas flow rate along the reactor may be caused by the changes in the temperature, pressure and total molar flow rate. In the present study, a differential reactor is considered as an example. The pressure drop through the reactor, in the actual experiment, is kept to less than 2% of the total pressure. The velocity gradient, $\partial U/\partial Z$, may be negligibly small because the differential reactor will produce only a small change in the total flow rate along the reactor length. The second term in Eq. (14) thus drops out and the following equation is obtained.

$$-\frac{U}{\rho_c R_g T}\frac{\partial P_A}{\partial Z}-(k_1 P_A\theta_{B_2}+k_2 P_A\theta_B{}^3+k_5 P_A\theta_B-k_{-5}\theta_{AB})$$
$$=\frac{\varepsilon}{\rho_c R_g T}\frac{\partial P_A}{\partial t} \tag{15}$$

Similarly, the corresponding equations for B_2, R, F and G are

$$-\frac{U}{\rho_c R_g T}\frac{\partial P_{B_2}}{\partial Z}-k_1 P_{B_2}\theta_v=\frac{\varepsilon}{\rho_c R_g T}\frac{\partial P_{B_2}}{\partial t} \tag{16}$$

$$-\frac{U}{\rho_c R_s T}\frac{\partial P_R}{\partial Z}+k_1 P_A \theta_{B_2}=\frac{\varepsilon}{\rho_c R_s T}\frac{\partial P_R}{\partial t} \tag{17}$$

$$-\frac{U}{\rho_c R_s T}\frac{\partial P_F}{\partial Z}+2k_3\theta_{\mathrm{In}}\theta_{B_2}^{2}=\frac{\varepsilon}{\rho_c R_s T}\frac{\partial P_F}{\partial t} \tag{18}$$

$$-\frac{U}{\rho_c R_s T}\frac{\partial P_G}{\partial Z}+2k_3\theta_{\mathrm{In}}\theta_{B_2}^{2}=\frac{\varepsilon}{\rho_c R_s T}\frac{\partial P_G}{\partial t} \tag{19}$$

The boundary conditions for Eqs. (15)~(19) are

$$P_A(Z,0)=P_{B_2}(Z,0)=f(Z) \tag{20}$$

$$P_R(Z,0)=P_F(Z,0)=P_G(Z,0)=g(Z) \tag{21}$$

$$P_A(0,t)=P_A{}^0,\ P_{B_2}(0,t)=P_{B_2}{}^0 \tag{22}$$

$$P_R(0,t)=P_R{}^0,\ P_F(0,t)=P_F{}^0,\ P_G(0,t)=P_G{}^0 \tag{23}$$

$$P_A(Z,t)=g(Z,t),\ P_A{}^{ns} \text{ at } Z=L \text{ as } t=\infty \tag{24}$$

$$P_{B_2}(Z,t)=g(Z,t),\ P_{B_2}{}^{ns} \text{ at } Z=L \text{ as } t=\infty \tag{25}$$

$$P_R(Z,t)=f(Z,t),\ P_R{}^{ns} \text{ at } Z=L \text{ as } t=\infty \tag{26}$$

$$P_F(Z,t)=f(Z,t),\ P_F{}^{ns} \text{ at } Z=L \text{ as } t=\infty \tag{27}$$

$$P_G(Z,t)=f(Z,t),\ P_G{}^{ns} \text{ at } Z=L \text{ as } t=\infty \tag{28}$$

Conditions (20) and (21) are the initial distribution of P_A and P_{B_2} for the reactants throughout the length of the reactor. Condition (22) indicates P_A and P_{B_2} at the inlet. Condition (23) states the amounts of products in the inlet of the reactor which are equal to zero in fact. Conditions (24)~(28) demonstrate the functional forms at the transient state, and they approach the steady states.

For steady state ($\partial P/\partial t=0$) eqs. (17), (18) and (19) become

$$\frac{U}{\rho_c R_s T}\left(\frac{dP_R}{dZ}\right)_{t=\infty}=k_1 P_A \theta_{B_2}=r_R \tag{29}$$

$$\frac{U}{\rho_c R_s T}\left(\frac{dP_F}{dZ}\right)_{t=\infty}=2k_3\theta_{\mathrm{In}}\theta_{B_2}{}^2=-2r_A=r_F \tag{30}$$

$$\frac{U}{\rho_c R_s T}\left(\frac{dP_G}{dZ}\right)_{t=\infty}=2k_3\theta_{\mathrm{In}}\theta_{B_2}{}^2=-2r_A=r_G \tag{31}$$

For the adsorbed phase, on the other hand, the material balance equations may be written by the functional form

$$\frac{\partial\theta_{B_2}}{\partial t}=f_1(P_A, P_{B_2}, \theta_{AB}, \theta_{B_2}, \theta_B, \theta_{\mathrm{In}})$$

$$=\frac{1}{q_m}(-k_1 P_A\theta_{B_2}-2k_3\theta_{\mathrm{In}}\theta_{B_2}{}^2+k_4 P_{B_2}\theta_v-k_6\theta_{B_2}\theta_v+k_{-6}\theta_{B_2}) \tag{32}$$

$$\frac{\partial\theta_B}{\partial t}=f_2(P_A, P_{B_2}, \theta_{AB}, \theta_{B_2}, \theta_B, \theta_{\mathrm{In}})$$

$$=\frac{1}{q_m}(k_1P_A\theta_{B_2}-3k_2P_A\theta_B{}^3+k_3\theta_{\mathrm{In}}\theta_{B_2}{}^2$$

$$-k_5P_A\theta_B+k_{-5}\theta_{AB}+2k_6\theta_{B_2}\theta_v-2k_{-6}\theta_B{}^2) \tag{33}$$

$$\frac{\partial\theta_{\mathrm{In}}}{\partial t}=f_3(P_A, P_{B_2}, \theta_{B_2}, \theta_B, \theta_{AB}, \theta_{\mathrm{In}})=\frac{1}{q_m}(k_2P_A\theta_B{}^3-k_3\theta_{\mathrm{In}}\theta_{B_2}{}^2) \tag{34}$$

$$\frac{\partial\theta_{AB}}{\partial t}=f_4(P_A, P_{B_2}, \theta_{B_2}, \theta_B, \theta_{AB}, \theta_{\mathrm{In}})=\frac{1}{q_m}(k_5P_A\theta_B-k_{-5}\theta_{AB}) \tag{35}$$

When the differential reactor is used (see Fig. 1), it has previously been confirmed that the concentration of reactants and products is linearly distributed along the reactor length. The arithmetic average $(\bar{P}_i, \bar{\theta}_i)$ thereby may be taken to be the averaged concentration of reaction components in the reactor. Equations (15)~(19) and (32)~(35) can be replaced by the ordinary differential equations, for the gas components

$$\frac{d\bar{P}_A}{dt}=-\frac{U}{\varepsilon}\frac{d\bar{P}_A}{dZ}-(k_1\bar{P}_A\bar{\theta}_{B_2}+k_2\bar{P}_A\bar{\theta}_B{}^3+k_5\bar{P}_A\bar{\theta}_B-k_{-5}\bar{\theta}_{AB}) \tag{36}$$

$$\frac{d\bar{P}_{B_2}}{dt}=-\frac{U}{\varepsilon}\frac{d\bar{P}_{B_2}}{dZ}-k_4\bar{P}_{B_2}\bar{\theta}_v \tag{37}$$

$$\frac{d\bar{P}_R}{dt}=-\frac{U}{\varepsilon}\frac{d\bar{P}_R}{dZ}+k_1\bar{P}_A\bar{\theta}_{B_2} \tag{38}$$

$$\frac{d\bar{P}_F}{dt}=-\frac{U}{\varepsilon}\frac{d\bar{P}_F}{dZ}+2k_3\bar{\theta}_{\mathrm{In}}\bar{\theta}_{B_2}{}^2 \tag{39}$$

$$\frac{d\bar{P}_G}{dt}=-\frac{U}{\varepsilon}\frac{d\bar{P}_G}{dZ}+2k_3\bar{\theta}_{\mathrm{In}}\bar{\theta}_{B_2}{}^2 \tag{40}$$

for the adsorbed components

$$\frac{d\bar{\theta}_{B_2}}{dt}=\frac{1}{q_m}(-k_1\bar{P}_A\bar{\theta}_{B_2}-2k_3\bar{\theta}_{\mathrm{In}}\bar{\theta}_{B_2}{}^2+k_4\bar{P}_{B_2}\bar{\theta}_v-k_6\bar{\theta}_{B_2}\bar{\theta}_v+k_{-6}\bar{\theta}_B{}^2) \tag{41}$$

$$\frac{d\bar{\theta}_B}{dt}=\frac{1}{q_m}(k_1\bar{P}_A\bar{\theta}_{B_2}-3k_2\bar{P}_A\bar{\theta}_B{}^3+k_3\bar{\theta}_{\mathrm{In}}\bar{\theta}_{B_2}{}^2-k_5\bar{P}_A\bar{\theta}_B+k_{-5}\bar{\theta}_{AB}$$

$$+2k_6\bar{\theta}_{B_2}\bar{\theta}_v-2k_{-6}\bar{\theta}_B{}^2) \tag{42}$$

$$\frac{d\bar{\theta}_{\mathrm{In}}}{dt}=\frac{1}{q_m}(k_2\bar{P}_A\bar{\theta}_B{}^3-k_3\bar{\theta}_{\mathrm{In}}\bar{\theta}_{B_2}{}^2) \tag{43}$$

$$\frac{d\bar{\theta}_{AB}}{dt}=\frac{1}{q_m}(k_5\bar{P}_A\bar{\theta}_B-k_{-5}\bar{\theta}_{AB}) \tag{44}$$

Using the conditions of the differential reactor, $d\bar{P}_j/dZ$ and $d\bar{P}_j/dt$ may approximately be written

$$\frac{d\bar{P}_j}{dZ}=\frac{\Delta P_j}{\Delta Z}=-\frac{P_j^0-P_j}{\mathrm{L}} \tag{45}$$

$$\frac{d\bar{P}_j}{dt}=\frac{d}{dt}\frac{P_j^0+P_j}{2} \tag{46}$$

Eq. (46) can also be rewritten as

$$\frac{d\bar{P}_j}{dt}=\frac{dP_j}{dt} \quad \text{for reactants} \tag{47}$$

$$\frac{d\bar{P}_j}{dt}=\frac{1}{2}\frac{dP_j}{dt} \quad \text{for products} \tag{48}$$

Because the conversion of reactants is less than a few percent and the concentration of products is zero at the inlet of the reactor. Accordingly the following equations rearranged for Eqs. (36)~(40) are obtained.

$$\frac{dP_A}{dt}=\frac{U}{\varepsilon L}(P_A^0-P_A)-(k_1P_A\theta_{B_2}+k_2P_A\theta_B{}^3+k_5P_A\theta_B-k_{-5}\theta_{AB}) \tag{49}$$

$$\frac{dP_{B_2}}{dt}=\frac{U}{\varepsilon L}(P_{B_2}{}^0-P_{B_2})-k_4P_{B_2}\theta_v \tag{50}$$

$$\frac{dP_R}{dt}=-\frac{2U}{\varepsilon L}\mathrm{P}_R+2k_1P_A\theta_{B_2} \tag{51}$$

$$\frac{dP_F}{dt}=-\frac{2U}{\varepsilon L}P_F+4k_3\theta_{\mathrm{In}}\theta_{B_2}{}^2 \tag{52}$$

$$\frac{dP_G}{dt}=-\frac{2U}{\varepsilon L}P_G+4k_3\theta_{\mathrm{In}}\theta_{B_2}{}^2 \tag{53}$$

For Eqs. (41)~(44), one can easily obtain similar equations replacing $\bar{P}_A$ and $\bar{P}_{B_2}$ by P_A and P_{B_2}. In addition, for the surface coverage θ_j, the following relation may be derived

$$\theta_A+\theta_{B_2}+\theta_{AB}+\theta_{\mathrm{In}}+\theta_v=1.0 \tag{54}$$

Since ordinary differential equations (41)~(44) and (49)~(53) are nonlinear, they must numerically be solved by the Runge-Kutta method, using a computer. The necessary reactor parameters, rate and equilibrium constants were arbitrarily determined from the references in past papers based on the actual reaction.[11] These parameters used in this study are listed in Tables 1 and 2.

Table 1. The reactor parameters

Reactor length	$L=77.0$ [cm]
Cross sectional area of reactor	$A(s)=0.385$ [cm^2]
Superficial gas velocity	$U=415$ [cm/min] (at 293 K)
Saturated amount of adsorbed species	$q_m=2.6\times10^{-6}$ [mol/g-cat]
Void fraction of packed bed reactor	$\varepsilon=0.53$ [−]
Catalyst bed density	$\rho_c=4.39$ [g/cm^3]
Temperature	$T=293$ [K]

Table 2. Summary of the rate constants

	Case 1	Case 2	Case 3
k_1 [mol/g-cat·min·atm]	1.5×10^{-5}	1.5×10^{-5}	1.5×10^{-5}
k_2 [mol/g-cat·min·atm]	1.6×10^{-5}	1.7×10^{-5}	1.4×10^{-5}
k_3 [mol/g-cat·min]	6.7×10^{-5}	6.7×10^{-5}	6.7×10^{-5}
k_4 [mol/g-cat·min·atm]	5.0×10^{-6}	4.6×10^{-6}	4.6×10^{-6}
k_5 [mol/g-cat·min·atm]	5.0×10^{-5}	5.0×10^{-5}	5.0×10^{-5}
k_{-5} [mol/g-cat·min]	1.5×10^{-5}	1.5×10^{-5}	1.5×10^{-5}
k_6 [mol/g-cat·min]	7.7×10^{-7}	8.2×10^{-3}	1.2×10^{-5}
k_{-6} [mol/g-cat·min]	8.0×10^{-6}	4.7×10^{-4}	6.9×10^{-7}
K_5 [atm^{-1}]	3.3	3.3	3.3
K_6 [−]	9.6×10^{-2}	18	18

3. Characterization of Steady State Functions

As is well known, the mode of steady state rate functions is sensitively affected by the kinetic structures which are specified by the reaction conditions and the characteristic nature of the catalysts used. One may choose three typical modes as examples with distinguishing features, as the following describes:

(1) Both R and F show a monotonic increase type with increasing P_A (Case 1)

(2) R shows a monotonic increase type whereas F shows a decrease type with increasing P_A (Case 2)

(3) Both R and F show a volcano type with increasing P_A (Case 3)

The three cases are characterized by the kinetic parameters presented in Table 2.

In Case 1, as can be seen in Fig. 2, the rate of R formation (r_R) is about ten times greater than the rate of F formation (r_F), and the former shows a typical monotonous increase mode whereas the latter shows an S-shape mode. The low value of r_F is due to the low value of θ_{In} which is less than 0.02 resulting from the value of k_2 being one fourth smaller than k_3. Comparing these modes, one may consider that the formation of R is due to a one step

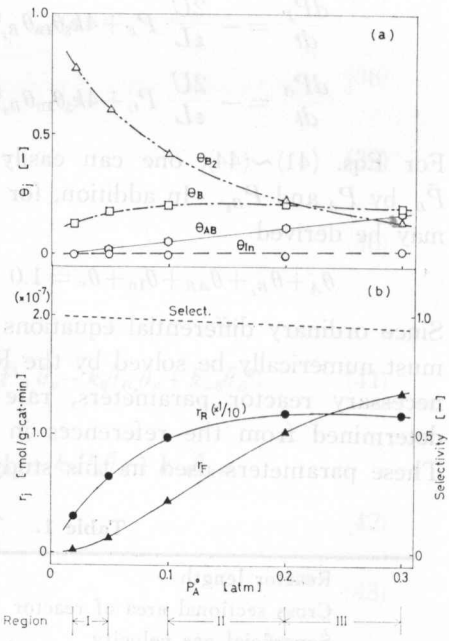

Fig. 2. (a) Plots of θ_j vs. P_A^0 in Case 1. (b) Plots of r_j vs. P_A^0 in Case 1; Conditions: see Tables. 1 and 2. I, II and III indicate three concentration regions.

reaction whereas F is formed through three steps Equations (5), (6) and (7). k_4 is the smallest of k_1-k_{-5}, which is why θ_{B_2} is steeply decreased with P_A.

In Case 2, as can be seen in Fig. 3, r_R shows a monotonous increase mode whereas r_F shows a monotonous decrease mode. Comparing the values of k_j presented in Table 2, the smallest is k_4 which is common with Case 1 and the largest is k_6 which is four orders larger than that in Case 1. The large value of k_6 decreases r_R which becomes of comparable order with r_F. The accumulation of (In) increasing θ_{In} induces a decrease mode of r_F resulting from the small coverage of active species $B_2 \cdot S$.

Case 3 presented in Fig. 4 demonstrates a typical volcano mode in both r_R and r_F. k_6 is an intermediate between Cases 1 and 2. θ_{In} is steeply increased up to 0.92 at $P_A=0.3$ atm which decreases the available surface coverage for the adsorption of B_2. This is the reason why both r_R and r_F show the volcano mode.

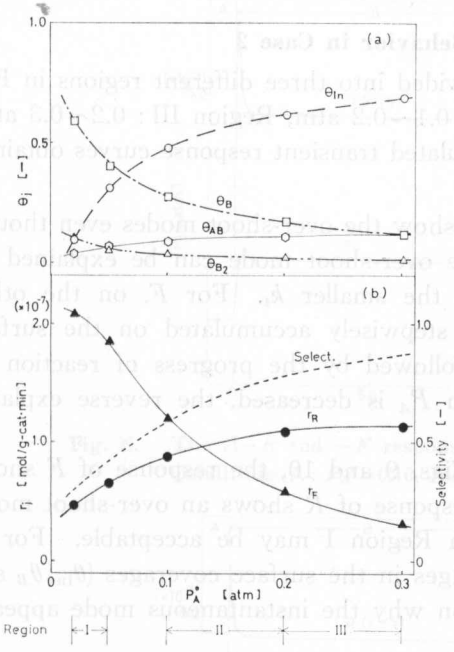

Fig. 3. (a) Plots of θ_j vs. $P_A{}^0$ in Case 2. (b) Plots of r_j vs. $P_A{}^0$ in Case 2; Conditions: see Tables. 1 and 2. I, II and III indicate three concentration regions.

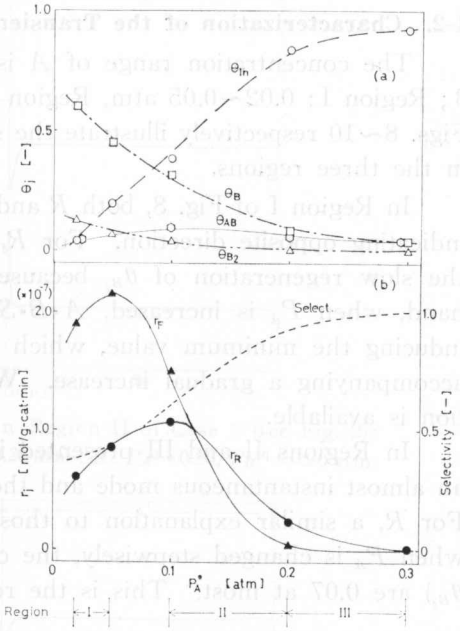

Fig. 4. (a) Plots of θ_j vs. $P_A{}^0$ in Case 3. (b) Plots of r_j vs. $P_A{}^0$ in Case 3; Conditions: see Tables. 1 and 2. I, II and III indicate three concentration regions.

4. Classification of the Transient Response Curves

4-1. Characterization of the Transient Behavior in Case 1

Computer simulation of the transient response has been carried out in three different regions of $P_A{}^0$ in Fig. 2; Region I: 0.02~0.05 atm, Region II: 0.1~0.2

atm, Region III: 0.2~0.3 atm. The simulated curves of Regions I, II and III are shown in Figs. 5~7, respectively.

Figs. 5 and 6 illustrate a typical over-shoot mode for R and a monotonic mode for F in Regions I and II. Fig. 7 illustrates a typical false start mode for both R and F. Thus, one may distinguish two groups, the over-shoot mode (Regions I and II) and false start mode (Region III). The over-shoot mode is due to the slow regeneration of active species $B_2 \cdot S$ from the gas phase resulting from the smaller value of k_4. The false start mode, on the other hand, is caused by the inhibition effect of the adsorption of A onto $B \cdot S$ to form a complex $A \cdot B \cdot S$ according to Equation (8). In Region III, the surface coverage of adsorbed components is within 0.5~0.6, and thereby the free surface for the adsorption of B_2 is less than $\theta=0.4$. In addition, the surface coverage of $B \cdot S$, θ_B, is unchanged as from 0.21 to 0.20 depending on the concentration of A whereas the change in θ_{AB} is from 0.12 to 0.18. This change usually becomes the characteristic false start mode in Region III.

4-2. Characterization of the Transient Behavior in Case 2

The concentration range of A is divided into three different regions in Fig. 3; Region I: 0.02~0.05 atm, Region II: 0.1~0.2 atm, Region III: 0.2~0.3 atm. Figs. 8~10 respectively illustrate the simulated transient response curves obtained in the three regions.

In Region I of Fig. 8, both R and F show the over-shoot modes even though indicating opposite direction. For R, the over-shoot mode can be explained by the slow regeneration of θ_{B_2} because of the smaller k_4. For F, on the other hand, when P_A is increased, $A \cdot B \cdot S$ is stepwisely accumulated on the surface inducing the minimum value, which is followed by the progress of reaction (6) accompanying a gradual increase. When P_A is decreased, the reverse explanation is available.

In Regions II and III presented in Figs. 9 and 10, the response of F shows an almost instantaneous mode and the response of R shows an over-shoot mode. For R, a similar explanation to those in Region I may be acceptable. For F, when P_A is changed stepwisely, the changes in the surface coverages (θ_{In}, θ_B and θ_{B_2}) are 0.07 at most. This is the reason why the instantaneous mode appears.

4-3. Characterization of the Transient Behavior in Case 3

Three different concentration regions of A are presented; in Fig. 4, Region I: 0.02~0.05 atm, Region II: 0.1~0.2 atm and Region III: 0.2~0.3 atm.Region I is at the right hand side of the maximum of $r_j - P_A$ plots, and Region II is at the left hand side of them.

In Region I, displayed in Fig. 11, F shows a typical false start mode whereas R shows an over-shoot mode. As described in sections 4-2 and 4-3, a similar explanation for both modes is available in the present case. The false start mode, however, appears at the lower concentration region of A whereas the mode previously appeared at the high concentration region of A as can be

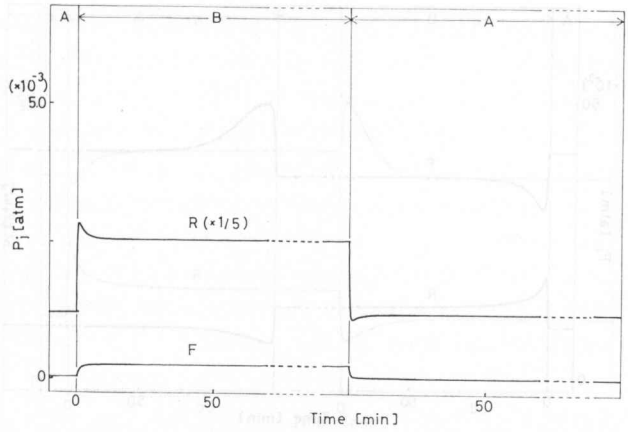

Fig. 5. The $A-R$ and $-F$ responses in Region I of Case 1 (see Fig. 2); Conditions A : $P_A{}^0=0.02$, $P_{B_2}{}^0=0.20$ atm ; B : $P_A{}^0=0.05$, $P_{B_2}{}^0=0.20$ atm.

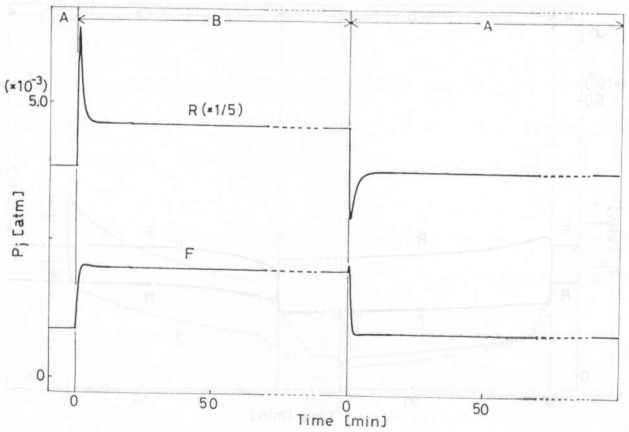

Fig. 6. The $A-R$ and $-F$ responses in Region II of Case 1 (see Fig. 2); Conditions A : $P_A{}^0=0.10$, $P_{B_2}{}^0=0.20$ atm ; B : $P_A{}^0=0.20$, $P_{B_2}{}^0=0.20$ atm.

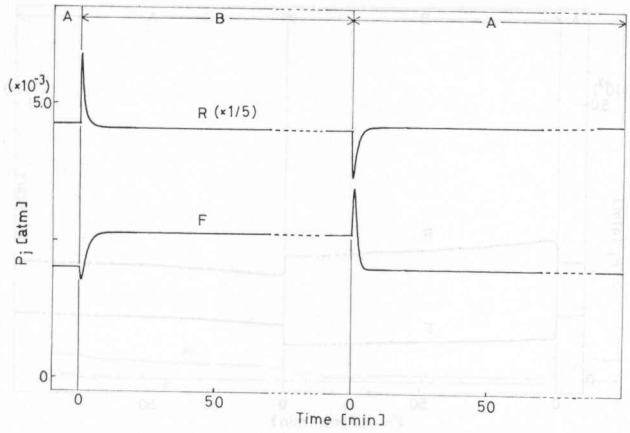

Fig. 7. The $A-R$ and $-F$ responses in Region III of Case 1 (see Fig. 2); Conditions A : $P_A{}^0=0.20$, $P_{B_2}{}^0=0.20$ atm ; B : $P_A{}^0=0.30$, $P_{B_2}{}^0=0.20$ atm.

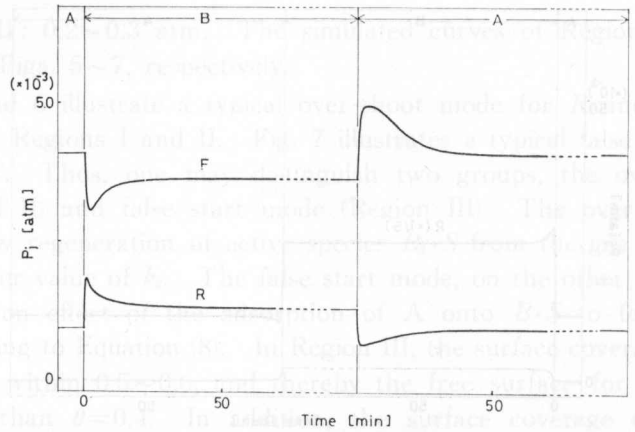

Fig. 8. The $A-R$ and $-F$ responses in Region I of Case 2 (see Fig. 3); Conditions A : $P_A{}^0=0.02$, $P_{B_2}{}^0=0.20$ atm ; B : $P_A{}^0=0.05$, $P_{B_2}{}^0=0.20$ atm.

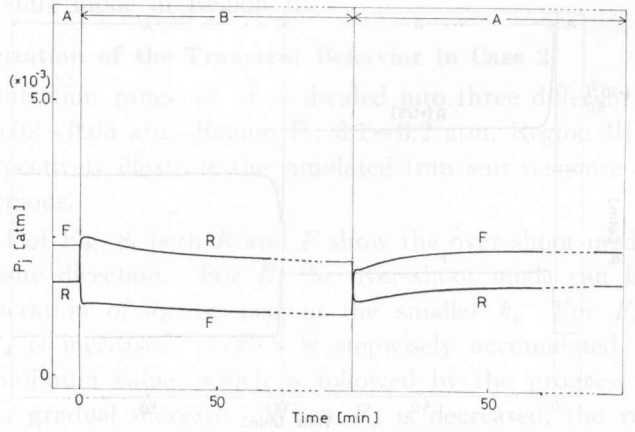

Fig. 9. The $A-R$ and $-F$ responses in Region II of Case 2 (see Fig. 3); Conditions A : $P_A{}^0=0.10$, $P_{B_2}{}^0=0.20$ atm ; B : $P_A{}^0=0.20$, $P_{B_2}{}^0=0.20$ atm.

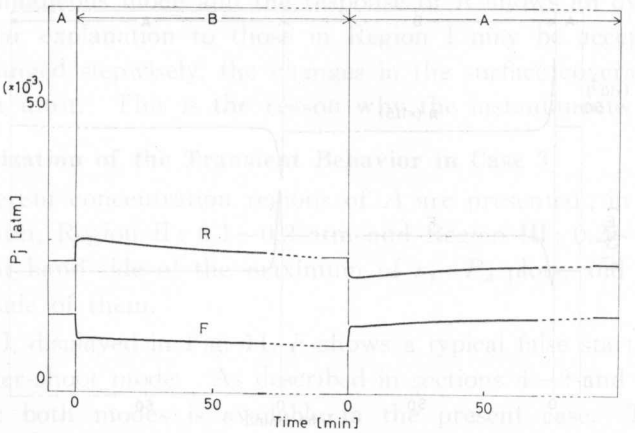

Fig. 10. The $A-R$ and $-F$ responses in Region III of Case 2 (see Fig. 3); Conditions A : $P_A{}^0=0.20$, $P_{B_2}{}^0=0.20$ atm ; B : $P_A{}^0=0.30$, $P_{B_2}{}^0=0.20$ atm.

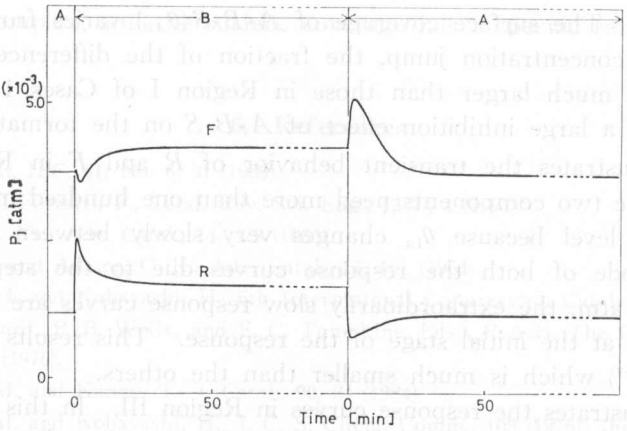

Fig. 11. The $A-R$ and $-F$ responses in Region I of Case 3 (see Fig. 4); Conditions A : $P_A{}^0=0.02$, $P_{B_2}{}^0=0.20$ atm ; B : $P_A{}^0=0.05$, $P_{B_2}{}^0=0.20$ atm.

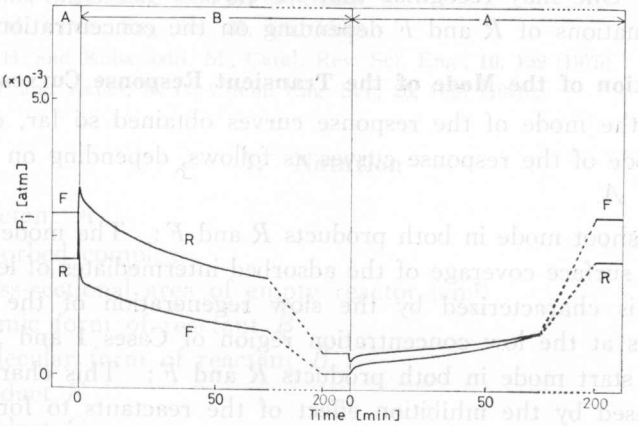

Fig. 12. The $A-R$ and $-F$ responses in Region II of Case 3 (see Fig. 4); Conditions A : $P_A{}^0=0.10$, $P_{B_2}{}^0=0.20$ atm ; B : $P_A{}^0=0.20$, $P_{B_2}{}^0=0.20$ atm.

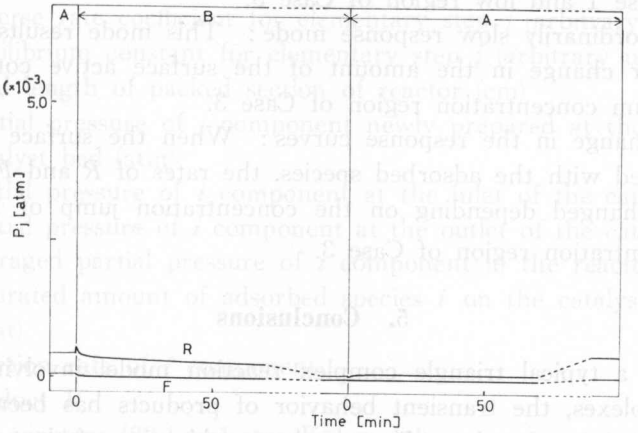

Fig. 13. The $A-R$ and $-F$ responses in Region III of Case 3 (see Fig. 4); Conditions A : $P_A{}^0=0.20$, $P_{B_2}{}^0=0.20$ atm ; B : $P_A{}^0=0.30$, $P_{B_2}{}^0=0.20$ atm.

seen in Fig. 7. The surface coverage of $A \cdot B \cdot S(\theta_{AB})$ varies from 0.03 to 0.06 caused by the concentration jump, the fraction of the difference ($\Delta\theta_{AB}$) is two. This change is much larger than those in Region I of Cases 1 and 2 ($\Delta\theta_{AB}=$ 0.016) resulting a large inhibition effect of $A \cdot B \cdot S$ on the formation of F.

Fig. 12 illustrates the transient behavior of R and F in Region II. The responses of the two components need more than one hundred minutes to reach a steady state level because θ_{In} changes very slowly between 0.38 and 0.85. Noting the mode of both the response curves due to the step change from $P_A=0.1$ to 0.2 atm, the extraordinarily slow response curves are obtained except for the change at the initial stage of the response. This results from the value of $k_{-6}(6.9\times10^{-7})$ which is much smaller than the others.

Fig. 13 illustrates the response curves in Region III. In this region, both r_R and r_F do not appreciably vary with the change in P_A. The response of R shows a slight false start mode whereas F shows no change depending on the change in P_A. One may recognize that no surface coverage is available to increase the formations of R and F depending on the concentration change of A.

4-4. Classification of the Mode of the Transient Response Curves

Based on the mode of the response curves obtained so far, one may easily classify the mode of the response curves as follows, depending on the concentration regions of A.

(1) Over shoot mode in both products R and F: The mode appears at the lower surface coverage of the adsorbed intermediates of less than $\theta=0.4$. This is characterized by the slow regeneration of the surface active species at the low concentration region of Cases 1 and 2.

(2) False start mode in both products R and F: This characteristic mode is caused by the inhibition effect of the reactants to form the inactive surface complexes, in which the proportion of the surface coverage change of the complexes is $\theta_{AB}\geq0.03$ at the high concentration region of Case 1 and low region of Case 3.

(3) Extraordinarily slow response mode: This mode results from a much slower change in the amount of the surface active complexes at the medium concentration region of Case 3.

(4) No change in the response curves: When the surface is almost fully covered with the adsorbed species, the rates of R and F formation are not changed depending on the concentration jump of A at the high concentration region of Case 3.

5. Conclusions

Based on a typical triangle complex reaction model involving some stable adsorbed complexes, the transient behavior of products has been classified into four characteristic modes depending on the combination of the values of kinetic parameters. The mode is sensitively characterized by the surface coverage of

far adsorbed complex, and the surface coverage has a specific range to show the four modes.

6. References

1) Adams, C. R., IEC, **61**, No. 6, 31 (1969).
2) Carra, S. and Forzatti, P., Catal. Rev. Sci. Eng., **15**(1), 1 (1977).
3) Margollis, L. Ya., Adv. Catal., **14**, 429 (1963).
4) Voge, H. H. and Adams, C. R., Adv. Catal., **15**, 151 (1964).
5) Kobayashi, M. and Kobayashi, H., 6th International Congress on Catalysis, London, 1976 (G. C. Bord, P. B. Wells, and F. C. Tompkins, Eds.), P. A 24, The Chemical Society, London, (1976).
6) Kobayashi, M. and Kanno, T., J. Catal., **90**, 24 (1984).
7) Kobayashi, M. and Kobayashi, H., J. C. S. Chem. Comm., 103 (1976); ibid., 77 (1977).
8) Kobayashi, M., "Catalysis Under Transient Conditions", 209, edited by A. T. Bell and L. L. Hegedus, ACS. (1982).
9) Kobayashi, M., Chem. Eng. Sci., **37**, 393 (1982).
10) Kobayashi, M., Chem. Eng. Sci., **37**, 403, (1982).
11) Kobayashi, H. and Kobayashi, M., Catal. Rev. Sci. Eng., **10**, 139 (1975).
12) Denis, G. H. and Kabel, R. L., Chem. Eng. Sci., **25**, 1057 (1970).

7. Notation

A : reactant A
$A \cdot B \cdot S$: adsorbed complex
$A(s)$: cross-sectional area of empty reactor (cm^2)
B : atomic form of reactant B
B_2 : molecular form of reactant B
F : product F
G : product G
In : surface intermediate
k_j : forward rate coefficient for elementary step j (arbitrary unit)
k_{-j} : reverse rate coefficient for elementary step j (arbitrary unit)
K_j : equilibrium constant for elementary step j (arbitrary unit)
L : total length of packed section of reactor (cm)
P_i^{ns} : partial pressure of i component newly prepared at the outlet of the catalyst bed (atm)
P_i^0 : partial pressure of i component at the inlet of the catalyst bed (atm)
P_i : partial pressure of i component at the outlet of the catalyst bed (atm)
$\bar{P}_i$: averaged partial pressure of i component in the reactor (atm)
q_m : saturated amount of adsorbed species i on the catalyst surface (mol/g-cat)
r_i : reaction rate of i component
R : product R
R_s : gas constant ($82.1\ cm^3 \cdot atm \cdot K^{-1} \cdot mol^{-1}$)
S : a catalytic site

t: time (min)
T: temperature (°K)
U: superficial gas velocity (cm/min)
U_i: interstitial gas velocity ($=U/\varepsilon$, cm/min)
Z: distance along reactor length (cm)

Greek letters

ε: void fraction of packed section of the reactor (dimensionless)
θ_i: fraction of catalyst monolayer covered with i component (dimensionless)
θ_v: fraction of vacant catalyst site a in monolayer (dimensionless)
$\bar{\theta}_i$: averaged surface coverage of i component (dimensionless)
π: total pressure (atm)
ρ_c: bulk catalyst density (g-cat/cm^3-reactor)
ρ_M: molar density (π/R_gT, mol/cm^3)